ELSEVIER

Polymer 42 (2001) 6503–6513

polymer

www.elsevier.nl/locate/polymer

Quasibinary and quasiternary styrene, dimethacrylate resin, and CTBN (or VTBN) liquid rubber systems: phase diagrams, interaction parameters and cured materials morphologies

María L. Auad, Mirta I. Aranguren, Julio Borrajo*

Institute of Materials Science and Technology (INTEMA), University of Mar del Plata, National Research Council (CONICET), Av. Juan B. Justo 4302, 7600 Mar del Plata, Argentina

Received 11 September 2000; received in revised form 28 December 2000; accepted 28 December 2000

Abstract

Four binary and two ternary experimental cloud point curves (CPC) for systems formulated with styrene (S), a dimethacrylate resin (DMAR), and poly(butadiene-co-acrylonitrile) liquid rubbers terminated in vinyl (VTBN) or carboxyl groups (CTBN), are presented. Measured CPCs of the binaries DMAR–CTBN, DMAR–VTBN and S–DMAR show upper critical solution temperature (UCST), while CPCs of the ternary S–DMAR–rubbers show liquid–liquid partial miscibility on the DMAR–rubber binary sides. A Flory–Huggins (F–H) thermodynamic analysis of the three measured binary cloud-point data allows the calculation of the respective interaction parameters and their temperature dependence. Interaction parameters for the other two binaries, S–CTBN (VTBN), were selected as the set of values that produced calculated spinodals, for the S–DMAR–rubbers ternaries, tangent to the respective experimental cloud-point diagrams at the critical point. The thermodynamic analysis was done taking into account the molecular polydispersity of CTBN, VTBN and DMAR components. Final morphologies of CTBN modified cured materials, obtained with two different molecular weight DMAR, were well correlated with the predicted miscibility for both systems. © 2001 Elsevier Science Ltd. All rights reserved.

Keywords: Dimethacrylate resins; Liquid rubbers; Cloud-point curves

1. Introduction

Dimethacrylate resins (DMAR) are some of the most important polyunsaturated monomers for composite formulations in industrial applications and in biomedical uses. The materials formulated with these resins show valuable properties, such as excellent resistance to corrosion and solvents, good adhesion, reasonably high glass transition temperature and modulus, as well as good electrical isolation [1]. As a consequence, these multifunctional unsaturated monomers have found a wide range of applications such as surface coating varnishes, coatings for printed circuits, aircraft and ship production, housing, ultraviolet cured inks, medical applications in dental and bone cements, etc. [2].

Like most thermosetting matrices, DMAR have been blended with several modifiers to improve their properties. For example, the impact properties of the cured S–DMAR thermosetting system have been improved by the addition of the liquid elastomers, carboxyl terminated poly(butadiene-co-acrylonitrile) (CTBN) and vinyl terminated poly(butadiene-co-acrylonitrile) (VTBN). These systems show heterogeneous morphologies constituted by domains rich in the S–DMAR copolymer and others domains rich in the additive [3,4]. As in the case of unsaturated polyester thermosets, during the curing of DMAR a high shrinkage of the materials occurs, that may produce several molding problems such as poor surface quality, dimensional changes, internal cracks, etc. that can be efficiently reduced by the use of low-profile additives (LPA) [5–8]. In most of these systems, the developed morphologies are formed by a mechanism denominated polymerization induced phase separation (PIPS). This mechanism appears when polymerization is started in a homogeneous mixture of comonomers and modifier. During the cure reaction, the system separates in two phases due to the presence of the new copolymer component, as well as the change of the relative concentrations of the comonomers and formed copolymer as the reaction proceeds and the degree of crosslinking increases. At the end of the reaction, most of the crosslinked

* Corresponding author. Tel.: +54-223-4816600; fax: +54-223-4810046.

E-mail address: jborrajo@fi.mdp.edu.ar (J. Borrajo).

0032-3861/01/$ - see front matter © 2001 Elsevier Science Ltd. All rights reserved.
PII: S0032-3861(01)00048-9

copolymer belongs to the major phase, while the additive is present in the minor phase. A complex combination of the liquid–liquid phase transition and the rate of cure reaction during polymerization results in the final network morphology and properties.

The understanding of the thermodynamic phase behavior of this reactive system is important for the development, production, and processing of polymeric materials with low-profile or toughening modifiers. During copolymerization, the reactive system is constituted by four components, S, DMAR, rubber additive and formed copolymer. At a given conversion, the phase transformation diagram is represented by a tetrahedron with one component in each vertex. The S–DMAR–rubber triangular face of the tetrahedron represents the phase behavior for the reactive system at zero conversion, meaning a ternary phase diagram for the physical mixture of the three components. The characteristics of the ternary phase diagram and the initial composition of the ternary homogeneous mixture, greatly determine the beginning of the phase separation by the PIPS mechanism, and the morphology generated during the copolymerization.

Studies on similar ternary reactive systems formulated with styrene, unsaturated polyester (UP) prepolymer and LPA, S–UP–LPA, demonstrate that the morphology developed can be correlated with the initial system miscibility, i.e. the position of the initial system in the ternary phase diagram [6,9–12]. Suspene et al. [6] have showed that the phase separation during copolymerization is mostly determined by the miscibility of S–UP binary, which presents lower miscibility than the other two pairs.

Poor DMAR–rubber or DMAR–LPA compatibility has been cited as a significant problem to achieve the suitable morphology to obtain toughening or low-profile effects [3,4,8]. However, no detailed studies of the initial miscibility of the modified systems, and the influence of the cure conditions on the phase separation process, are available from the literature.

In general, miscibilities in binary and ternary physical mixtures are severely affected by the molecular properties of each component, such as molecular weight, polydispersity, chemical copolymer composition, the presence of specific chain end groups and molecular association [13–19]. Liquid–liquid phase diagrams for systems formulated with styrene, DMARs and the liquid rubbers CTBN or VTBN have not been previously reported. The thermodynamic analysis of ternary phase diagrams needs that the interaction parameters of the corresponding three binaries S–DMAR, DMAR–CTBN (or VTBN), and S–CTBN (or VTBN) have been previously determined. The simplest way to calculate these parameters is to apply the F–H lattice theory to the analysis of the quasibinary and quasiternary cloud point curves (CPCs) measurements [17,18,20,21].

In this paper, the initial miscibility of the unreacted system is measured and modelled. The miscibilities of the binaries S–DMAR and DMAR–CTBN (VTBN) as well as the ternaries S–DMAR–CTBN (VTBN) at 50 and 70°C were determined by measuring their CPCs which were further analyzed with the F–H lattice theory.

In the first part of this work, the determination of the χ-parameter equations for all the binaries system is discussed. The ternary diagrams were calculated from the binary interaction parameters. A brief discussion of the final morphology and its relation to the initial miscibility of the system is also included. A thermodynamic model capable of explaining the morphologies developed during the cure reaction of S–DMAR and S–DMAR–CTBN systems will be presented in a following paper.

2. Theoretical background

Different polymer-solution theories have been developed during the last fifty years, the best known is the F–H lattice theory, originally developed to describe polymer binary solutions behavior [13]. Tompa [14] was the first to extend the theory to ternary systems. Later, different authors [15,22–29] have done a detailed analysis on the dependence of the CPC, shadow curves (ShC), coexistence curves (CC), spinodal curves (SC) and critical solution point (CSP) in quasibinary and quasiternary polymer solutions with the relative molar volumes of the components, polydispersities and types of polymer molecular weight distributions.

In this study, the simplest version of F–H lattice theory was applied considering the binary interaction parameters as composition independent and inversely proportional to temperature, and taking in account the effect of each component polydispersity. However, despite its simplicity, this thermodynamic model is still suitable to obtain valuable quantitative information from these complex systems.

The expression derived from the F–H theory for the dimensionless mixing Gibbs free energy per mole of lattice sites in a multicomponent system with polydisperse polymers is given by the following equation [15]:

$$\Delta\overline{G^{\mathrm{mix}}} = \frac{\Delta G^{\mathrm{mix}}}{MRT} = \sum_i \sum_{j=1}^{N_i} \frac{\phi_{ij}}{r_{ij}} \ln \phi_{ij} + \sum_{i<k} \chi_{ik}\phi_i\phi_k. \qquad (1)$$

The symbols i, $k = 1, 2, 3$ represent components; $j = 1, 2, \ldots, N_i$ the polymerization degree of different molecular species corresponding to the i component molar mass-fraction distribution; ϕ_{ij} is the volumetric fraction of the j molecular specie of the i component and $\phi_i = \sum_j \phi_{ij}$ is the volumetric fraction of the i component; $\chi_{ik} = \chi_{ki}$ is the composition independent binary interaction parameter. M factor is given by

$$M = \sum_i \sum_{j=1}^{N_i} n_{ij} r_{ij}, \qquad (2)$$

which represents the mole number of lattice sites in the system; n_{ij} is the number of moles of the ij molecular specie

and r_{ij} its relative molar volume, defined by

$$r_{ij} = \frac{V_{ij}}{V_r}. \tag{3}$$

In this equation, V_{ij} is the molar volume of the j molecular specie of the i component, and V_r is the reference volume, usually taken as the molar volume of the smaller component or the smaller polymer monomeric unit.

The mass balance for all the ij species in the mixture gives

$$\sum_i \sum_{j=1}^{N_j} \phi_{ij} = \sum_i \phi_i = 1. \tag{4}$$

From Eq. (1), the dimensionless chemical potential difference per mole of lattice sites, between a generic ij molecular specie in the solution and in the pure state, is given by its definition

$$\frac{\Delta\mu_{ij}}{r_{ij}RT} = \left[\frac{\partial(\Delta G^{mix}/MRT)}{\partial n_{ij}} \right]_{P,T,n_{km\neq ij}}. \tag{5}$$

The expression for $\Delta\mu_{ij}$ of a ij molecular specie in the mixture is given by the following general equation, valid for a binary or ternary system

$$\frac{\Delta\mu_{ij}}{r_{ij}RT} = \frac{1}{r_{ij}} + \frac{\ln \phi_{ij}}{r_{ij}} - \sum_i \sum_{j=1}^{N_i} \frac{\phi_{ij}}{r_{ij}} + \sum_{k\neq i} \chi_{ik}\phi_k(1-\phi_i) - \chi_{kl}\phi_k\phi_l, \tag{6}$$

where $i(k,l) = 1,2,3$ are the components in a ternary system, and $i(k) = 1,2$ with $\phi_l = 0$ in a binary. It can be seen that the third and fourth term in the second side of this equation are determined by the global composition, ϕ_i.

The spinodal curve (SC) in a multicomponent system represents the stability limit of the one phase homogeneous mixture. Inside this limiting curve the mixture must be separated in two phases. The SC thermodynamic requirement, at constant pressure and temperature, is that the determinant of the square matrix of the second derivatives of the molar Gibbs free energy with respect to the independent composition variables, be identical to zero

$$\left|\Delta\overline{G^{\mathrm{mix}}}''\right| = 0 \qquad P \text{ and } T \text{ are constants.} \tag{7}$$

The determinant dimension is fixed by the total number of molecular species [15], $(N_1 + N_2 + N_3 - 1) \times (N_1 + N_2 + N_3 - 1)$, and the result for a ternary system with three polydisperse components is given by Eq. (8)

$$\left(\frac{1}{r_{1w}\phi_1} + \frac{1}{r_{2w}\phi_2} - 2\chi_{12}\right)\left(\frac{1}{r_{1w}\phi_1} + \frac{1}{r_{3w}\phi_3} - 2\chi_{13}\right) - \left(\frac{1}{r_{1w}\phi_1} + \chi_{23} - \chi_{12} - \chi_{13}\right)^2 = 0. \tag{8}$$

For a binary mixture of two polydisperse polymers, the SC curve is given by Eq. (9)

$$\frac{1}{r_{1w}\phi_1} + \frac{1}{r_{2w}\phi_2} - 2\chi_{12} = 0. \tag{9}$$

In these equations, r_{iw} is the weight average relative molar volume. In a binary or ternary mixture of polydisperse polymers, the spinodal curve is unique and retains the same shape and significance than in a true binary or ternary system, it only depends on weight average relative molar volume and not on the polymer polydispersity. That means that a quasibinary (or a quasiternary) system of polydisperse polymers has the same SC that a true binary (or true ternary) system of monodisperse polymers with the same average relative molar volumes than those of the polydisperse system.

At the CSP, in addition to Eq. (7), it must be simultaneously satisfied that the determinant of square matrix of the third derivatives of the molar Gibbs free energy with respect to the composition of each molecular specie, be also zero [15]

$$\left|\Delta\overline{G^{\mathrm{mix}}}'''\right| = 0 \qquad \text{at constant } P \text{ and } T. \tag{10}$$

As in the SC analysis, for a ternary mixture of three polydisperse components the CSP composition shows dependence with the polymer average relative molar volumes and the three pair interaction parameters [15]

$$\begin{aligned}
&\frac{r_{1z}}{(r_{1w}\phi_1)^2} \times \left(\frac{1}{r_{2w}\phi_2} + \chi_{13} - \chi_{12} - \chi_{23}\right)^3 \\
&\times \left(\frac{1}{r_{3w}\phi_3} + \chi_{12} - \chi_{13} - \chi_{23}\right)^3 + \frac{r_{2z}}{(r_{2w}\phi_2)^2} \\
&\times \left(\frac{1}{r_{3w}\phi_3} + \chi_{12} - \chi_{13} - \chi_{23}\right)^3 \\
&\times \left(\frac{1}{r_{1w}\phi_1} + \chi_{23} - \chi_{12} - \chi_{13}\right)^3 + \frac{r_{3z}}{(r_{3w}\phi_3)^2} \\
&\times \left(\frac{1}{r_{2w}\phi_2} + \chi_{13} - \chi_{12} - \chi_{23}\right)^3 \\
&\times \left(\frac{1}{r_{1w}\phi_1} + \chi_{23} - \chi_{12} - \chi_{13}\right)^3 = 0.
\end{aligned} \tag{11}$$

Similarly, the corresponding expression for a binary mixture of two polydisperse polymers is

$$\frac{r_{1z}}{(r_{1w}\phi_1)^2} - \frac{r_{2z}}{(r_{2w}\phi_2)^2} = 0. \tag{12}$$

In all the previous equations, parameters r_{in}, r_{iw} and r_{iz} are the number, weight and zeta, averages of the relative molar volumes of all j molecular species in the i polymer component distribution. In the framework of the Flory–Huggins (F–H) lattice theory, the three averages determine different properties of the phase diagram; r_{in} determines the cloud

point and coexistance curves; r_{iw} the SC and both r_{iw} and r_{iz}, the CSP.

3. Experimental

3.1. Materials

A low molecular weight dimethacrylate resin, DMAR(583), was synthesized by reacting an epoxy resin, diglicidyl ether of bisphenol A (DGEBA MY 790, Ciba Geigy, equivalent weight 176.2 g/equiv.), with methacrylic acid (Norent Plast S.A., laboratory grade reagent) using triphenylphosfine as catalyst (Fluka A.G., analytical reagent). Final conversion reached was higher than 93% for all batches. Synthesized DMAR(583) was stabilized with 300 ppm of hydroquinone [30,31]. A high molecular weight commercial dimethacrylate resin, DMAR(1015) (PALATAL A 430 BASF AG) was used during the study of the S–DMAR binary.

Molecular weights were measured by size exclusion chromatography (SEC) using oligomer fractionation columns. Although a polystyrene calibration was used, the measured molecular weight for the DMAR(583) was in very good agreement with the value estimated from the initial reactants ($M_{\mathrm{n\ calc.}} = 517$ g/mol). Similarly, the value measured for the commercial DMAR is in agreement with values reported in the literature [8]. The SEC technique also allowed to obtain the polydispersity index for all the initial samples.

The two liquid rubbers used as additives were copolymers of butadiene and acrylonitrile (BF Goodrich), which had either carboxyl end groups (CTBN, 1300×8) or vinyl end groups (VTBN, 1300×8).

Table 1 summarizes the molecular parameters and the density experimentally measured for all the components used in the thermodynamic study.

The final morphologies were observed in samples of DMAR crosslinked with styrene and with added rubbers. The reaction was initiated by an amine-accelerated system using benzoyl peroxide (Luzidol 75%, Akzo Chemicals S.A.) as initiator and *N*,*N*-dimethyl aniline (Akzo Chemicals S.A.) as promoter. All the materials were used as received.

3.2. Cloud-point curve determination

A series of binary mixtures with different compositions were prepared and introduced in a cell with controlled temperature programs. The cell was a glass cylinder-with-jacket of 10 cm^3 capacity. The fluid circulating in the jacket was supplied from an external bath at programmable heating rates. A rate of 2°C/min was used in the heating and cooling programs. Cloud point temperatures of each binary solution were determined by averaging the measured values of the onset of turbidity during cooling and the onset of transparency during heating. The solutions were thoroughly stirred during measurements to assure that the temperature was uniform throughout the sample.

For ternary systems, cloud point compositions were obtained by a simple titration method. Initially heterogeneous fluid mixtures of two or three components of known global concentrations were prepared. A fixed volume of this mixture was introduced in the glass cell equipped with a magnetic stirring bar. At a constant temperature, these solutions were titrated with liquid styrene, that acts as solvent of the heterogeneous mixture. In all cases, the styrene was added to the initial mixture from a burette with 0.1 cm^3 precision. The measurement of the amount of liquid styrene required to achieve the onset of transparency in the initially heterogeneous mixture, allows the calculation of the final system composition. In this work, the system composition at the transparency-point was taken as same as that corresponding to the ternary cloud-point. These final global compositions, expressed as volumetric fractions, generate the cloud-point curve (CPC) in a ternary phase diagram.

3.3. Electron microscopy

Plates of 2 mm of thickness were molded from 40.5%S–49.5%DMAR(583)–10%CTBN and 40.5%S–49.5%DMAR(1015)–10%CTBN resin mixtures. The samples were isothermaly cured for 2 h at 30°C and post-cured at 170°C during 1 h. Concentrations of benzoyl peroxide and dimethyl aniline were 3 and 0.3%, respectively. Fractured specimens were gold coated and then observed by scanning electron microscopy (SEM). Samples

Table 1
Physicochemical characteristics of the used components

	Styrene (S) (1)	DMAR (2) synthesized	DMAR (2) commercial	CTBN (3)	VTBN (3)
M_n (g/mol)	104	583[a]	1015[a]	3600[b]	3600[b]
DI	1	1.06	1.74	1.81	1.81
Density ρ (g/cm^3) (25°C)	0.89	1.16	1.16	1.06	1.06
r_n	2.05	8.82	16.51	59.62	59.62
r_w	2.05	8.82	28.19	107.67	107.62
r_z	2.05	8.82	54.82	155.7	155.62

[a] Measured by SEC, THF solvent at 1 ml/min.
[b] Taken from the supplier's catalog.

to be studied by transmission electron microscopy (TEM) were previously stained with OsO_4 (immersed in OsO_4 solution during 7 days). Then a thin slice was obtained by microtoming the specimen to be observed by TEM. Only the unreacted C=C bonds are stained by this technique. Since the DMAR and S are already reacted through their unsaturations, only the less reactive internal unsaturations of the butadiene comonomer in the liquid rubbers are stained. Electronic microscopy was carried out using a Jeol JSM 35 CF microscope.

4. Results and discussion

Usually, phase diagrams for quasibinary or quasiternary systems are presented using two sets of coordinates T–ϕ_1 and ϕ_1–ϕ_2, respectively. They are different projections of the T–P–ϕ_i hypersurfaces representing different states of polymer fractionation during the liquid–liquid macrophase separation of these systems. As a consequence, the CPC and the shadow-curve (ShC), that represent the onset of phase separation in the system, do not superimpose with any of the coexistence curves (CCs), that would represent the system at different degrees of macrophase separation.

Under constant temperature and pressure, thermodynamic requirements for liquid–liquid phase equilibrium, at the cloud-point or coexistence conditions, in a mixture with polydisperse components are given by the following equations:

$$\Delta\mu_{ij}^{\alpha} = \Delta\mu_{ij}^{\beta}, \tag{13}$$

where α and β represent the mother and emergent phases in equilibrium at the cloud point conditions, respectively, or the equilibrium coexistence phases during macrophase separation.

Numerical methods to analyze and calculate CPCs, ShCs, SCs, CSPs and CCs, in mixtures with polydisperse components have been proposed and discussed in the literature [15,23–28]. The procedure developed by Kamide et al. for quasibinary [29] and quasiternary [18] solutions was used in this study.

4.1. Quasibinary systems

4.1.1. DMAR(583)(2)–CTBN(3) and DMAR(583)(2)–VTBN(3)

Figs. 1 and 2 show experimental CPCs diagrams for systems formulated with DMAR(583) and two liquid rubbers CTBN and VTBN, respectively. An upper-critical solution behavior is observed in both CPCs.

In order to apply the F–H theory to these systems, it is necessary to define the reference volume for the unit cell. Based in previous studies on systems with the same type of liquid rubbers, the value $V_r = 59.962\ cm^3/mol$ corresponding to the acrylonitrile rubber comonomer was adopted [32,33].

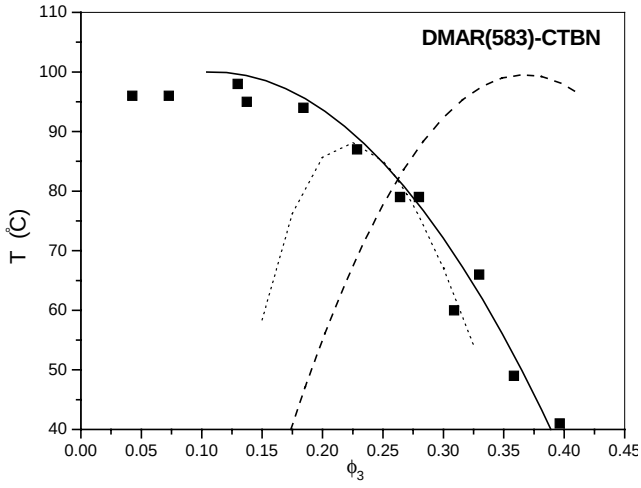

Fig. 1. DMAR(583)–CTBN quasibinary system: ■ experimental cloud-point data; — calculated cloud-point curve; - - - calculated shadow curve; ··· spinodal curve.

At the cloud-point, the use of the general phase equilibrium condition (13) together with expression (6) for the chemical potential of a *ij* generic molecular specie, leads to the equations for equilibrium calculation in the DMAR(583)–CTBN or DMAR(583)–VTBN quasibinary systems. For the rubber component, the expression is

$$\sigma_3 - \left[\left(\frac{\phi_2}{r_2} + \frac{\phi_3}{r_{3n}}\right)^{\beta} - \left(\frac{\phi_2}{r_2} + \frac{\phi_3}{r_{3n}}\right)^{\alpha}\right] + \chi_{23}\left[\left(\phi_2^{\beta}\right)^2 - \left(\phi_2^{\alpha}\right)^2\right] = 0. \tag{14}$$

For the DMAR(583) component, a similar equation with changed subindex holds. Here, σ_3 (or σ_2) is the separation factor, its value determines the fractionation extension of

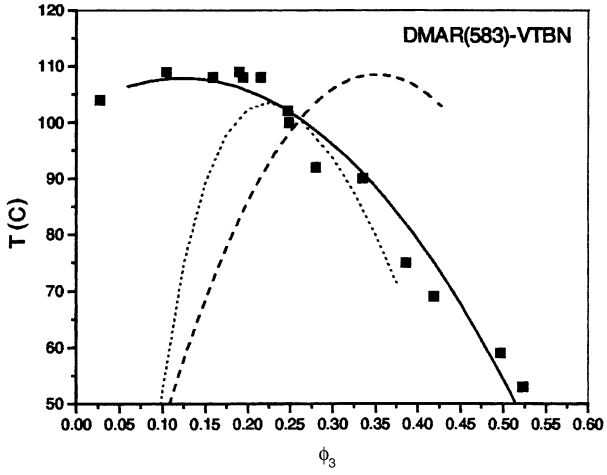

Fig. 2. DMAR(583)–VTBN quasibinary system: ■ experimental cloud-point data; — calculated cloud-point curve; - - - calculated shadow curve; ··· spinodal curve.

each molecular specie of the rubber component between the two equilibrium phases. In the framework of F–H theory, the separation factor depends only on number average relative molar volumes, r_{in}, and components compositions in both equilibrium phases, $\phi_i^{\alpha,\beta}$. As a consequence, at a given pressure and temperature, σ_3 has the same value for all the $3j$ molecular species included in the rubber distribution function, W_{3j}. Its definition is

$$\sigma_3 = \frac{1}{r_{3j}} \ln \frac{(\phi_{3j})^{\beta}}{(\phi_{3j})^{\alpha}}, \tag{15}$$

where $\phi_{3j}^{\alpha} = W_{3j}\phi_3^{\alpha}$ and $\phi_{3j}^{\beta} = W_{3j}\phi_3^{\alpha} e^{\sigma_3 r_{3j}}$.

This distribution corresponds to that of the mother α phase, since at the cloud point condition, only an infinitesimal amount of rubber is in the emergent phase. The Schulz–Zimm distribution function was used in this work, its expression for the two rubbers is given by the following equation:

$$W_{3j} = \frac{y^{h+1}}{\Gamma(h+1)} r_{3j}^{h} \exp(-y r_{3j}), \tag{16}$$

where $y = h/r_{3n}$ and $h = ((r_{3w}/r_{3n}) - 1)^{-1}$. The values for the number and weight relative molar volume averages for the rubbers, r_{3n} and r_{3w}, are given in Table 1. As can be also observed in Table 1, DMAR(583) has a low polydispersity index (DI = 1.06), for this reason it is considered as monodisperse in the calculations.

In addition to Eq. (14), written for each of the two components of the mixture, a mass balance for the emergent β phase must be included in this analysis. This balance is given by the equation:

$$\sum_{j=1}^{N_3} \phi_3^{\alpha} W_{3j} \exp(r_{3j}\sigma_3) + \phi_2^{\alpha} \exp(r_2\sigma_2) = 1. \tag{17}$$

The experimental cloud point phase diagram (T vs. ϕ_i) was analyzed with Eqs. (14)–(17) to obtain the interaction parameter and the composition of the emergent β phase, at each temperature. ShC is represented by the locus of emergent β phase compositions. During the calculation, the rubber molecular mass-fraction distribution, given by Eq. (16), were truncated at $r_{3j} = 800$ (molecular weight $M_{3j} = 50,800$), because truncation at higher values did not change the results.

Calculated values of the interaction parameter are represented in Table 2 for both quasibinary systems. Continuous lines in Fig. 3 represent χ vs.$1/T$ behavior fitted linearly as

$$\chi_{23} = a + \frac{b}{T(K)}. \tag{18}$$

Table 2
Constants a and b of the interaction parameter equation

Binary pair	a	b (K)
S–DMAR	−0.161	158.516
S–CTBN	−0.194	44.316
S–VTBN	−0.306	94.171
DMAR–VTBN	−0.0058	37.479
DMAR–CTBN	−0.051	15.561

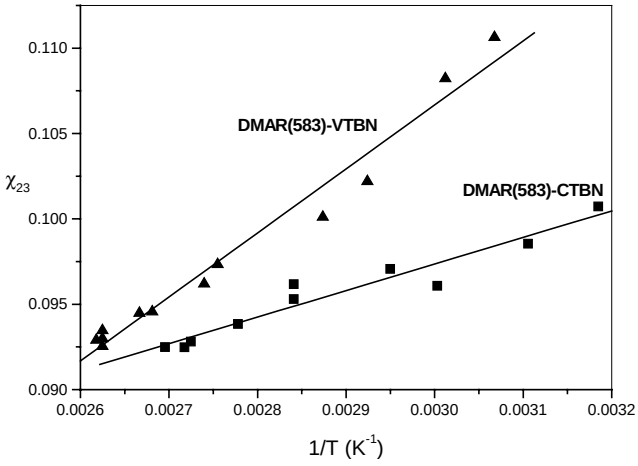

Fig. 3. Temperature dependence of the interaction parameters: (a) DMAR(583)–VTBN quasibinary systems; (b) DMAR(583)–CTBN quasibinary system; ■ values calculated from the experimental cloud-point data; — results of the linear regression equation.

Figs. 1 and 2 show that miscibility of DMAR(583)–VTBN system is lower than that of DMAR–CTBN. This observation is well correlated with calculated values for the interaction parameters in both systems, $\chi(T)_{\text{DMAR–VTBN}} > \chi(T)_{\text{DMAR–CTBN}}$. Since the relative sizes of both rubbers are essentially the same, the different miscibility behavior of these systems can be explained by the only difference between both liquid rubbers, their chain ends groups. Presumably, the favorable dipolar interactions between the terminal carboxyl end groups of the CTBN and the ester and alcoholic groups of the DMAR improve the miscibility of the DMAR–CTBN system in comparison with the less favorable interactions between the terminal vinyl groups of the VTBN and the polar groups of the DMAR in the DMAR–VTBN system. The best fitting parameters of Eq. (18) for the quasibinary systems are given in Table 2.

Calculated CPCs, ShCs and SCs for both systems are shown in Figs. 1 and 2, they were obtained using $\chi(T)$ values given by Eq. (18) from the inverse calculation. Comparing experimental and calculated CPCs, it can be concluded that this χ-parameter equation describes quite well the experimental quasibinary cloud-point phase diagrams for these systems.

Fig. 4 shows the emergent β phase normalized mass-fraction distribution function for VTBN molecular species, as a function of their relative molecular volume, r_{3j}. Each curve in this figure represents the VTBN mass-fraction distribution for a point of the shadow curve in Fig. 2. At the critical temperature, $T = T_c$, the emergent phase has the

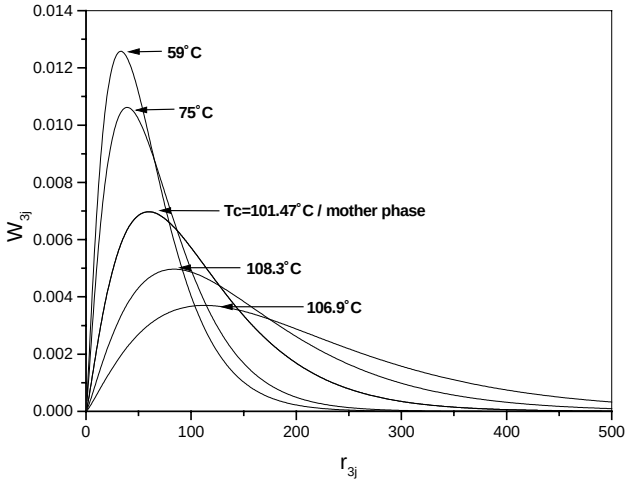

Fig. 4. Calculated molecular mass fraction distribution for VTBN in the emergent phase, in function of their relative molecular volumes at different temperatures 59, 75, 108.3, 106.9, 101.5°C.

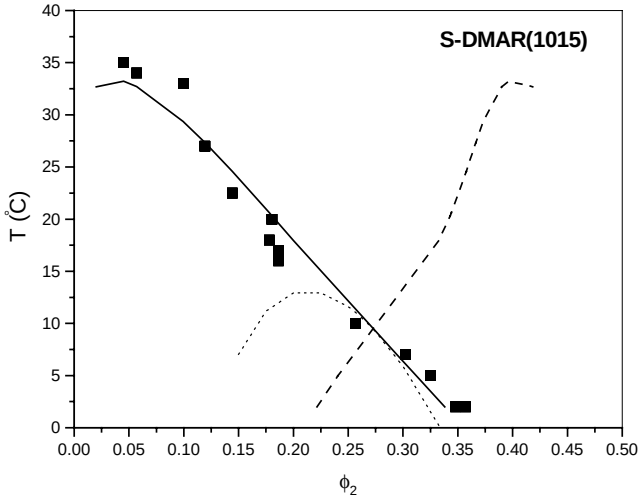

Fig. 5. S–DMAR(1015) quasibinary system: ■ experimental cloud-point data; — calculated cloud-point curve; - - - calculated shadow curve; ⋯ spinodal curve.

same distribution than the mother phase. At temperatures lower than the critical conditions, $T < T_c$, the emergent phase shows a narrow distribution rich in low molecular weight VTBN species ($M_n^{\beta} < M_n^{\alpha}$). At temperatures higher than critical condition, $T > T_c$, the emergent phase presents a broad distribution rich in high molecular weight VTBN species ($M_n^{\beta} < M_n^{\alpha}$). The rubber polydispersity affect the liquid–liquid phase diagram causing molecular fractionation from the α-mother phase toward the β-emergent one. As a consequence, the rubber component has different average molecular properties in each equilibrium phase.

4.1.2. S(1)–DMAR(1015)(2)

Cloud-points corresponding to the liquid–liquid phase separation in S–DMAR(583) solutions could not be measured during cooling, due to the DMAR(583) low molecular weight. Instead, a solid–liquid transition is observed at temperatures below the melting point of styrene, 242 K, at which solid styrene is separated from DMAR(583) liquid solution. On the other hand,S–DMAR(1015) solutions showed measurable cloud-points below room temperature.

In the framework of the F–H theory, binary interaction parameters are only temperature dependent and not concentration or molecular weight dependent. Under this assumption, it is possible to assign to the unmeasured binary S–DMAR(583) the same χ-parameter calculated from the experimental CPC measured on S–DMAR(1015) solutions. Fig. 5 shows the experimental CPC measured for this binary system.

The calculation of the χ-parameter for this system, requires the previous knowledge of the molar mass-fraction distribution of DMAR(1015). As can be observed in Fig. 6, the size exclusion chromatogram (SEC) of this resin shows a wide molecular weight distribution, with narrow peaks in the low molecular weight region, and a long tail at high molecular weights. This feature requires that DMAR(1015) be considered as a polydisperse component in the thermodynamic calculations. Because of the complex experimental molecular weight distribution, a discrete distribution including 40 pseudo-species was introduced in the model instead and it is shown in Fig. 6 as a bar plot. The average molecular weights M_n, M_w and M_z calculated with the discrete distribution are in very good agreement with those measured by SEC.

The constants a and b (Eq. (18)), for this quasibinary system are given in Table 2. Inverse calculation of CPC, ShC and SC was performed using the expression found for

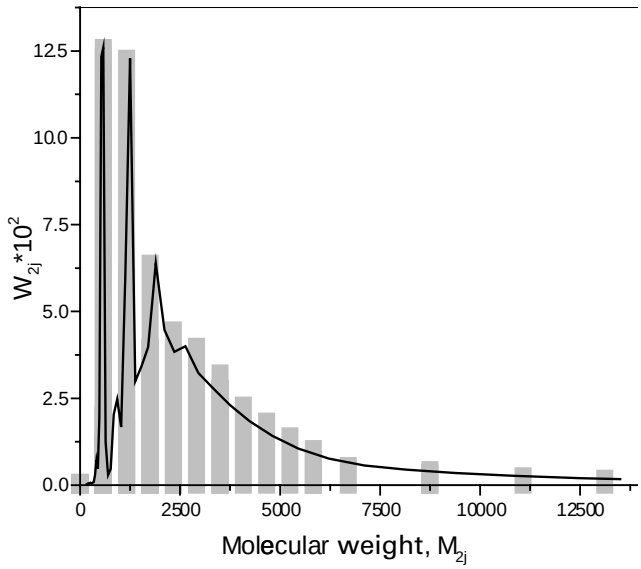

Fig. 6. DMAR(1015) mass fraction distribution as a function of the molecular weights: — actual SEC distribution; bars: pseudocomponents discrete distribution.

the χ-parameter. The curves plotted in Fig. 5 represent the results of the calculations. As can be seen, experimental and calculated CPCs show very good agreement. The ability of this $\chi(T)$ equation to represent the S–DMAR(583) interaction parameter correctly was further confirmed by successfully using it in the analysis of the ternary systems CPC.

4.1.3. S(1)–CTBN(3) and S(1)–VTBN(3)

As in the S–DMAR(583) system, the cloud-points corresponding to the liquid–liquid phase separation in S–CTBN and S–VTBN solutions could not be measured during cooling, due to the high solubility of the S–CTBN and S–VTBN systems. Consequently, the solidification of S takes place before any liquid–liquid phase separation occurs.

At a constant temperature and pressure, the CPC and SC of any ternary system are tangent at the critical point. This property was used to calculate χ_{13} from the experimental data of the S–DMAR(583)–CTBN and S–DMAR(583)–VTBN quasiternary systems.

Simultaneous solution of Eqs. (8) and (11) allows us to calculate the quasiternary critical composition, ($\phi 1c$, $\phi 2c$), for a given system at a selected temperature. A trial and error method was used to find the χ_{13} value that allows to calculate a SC curve tangent to the experimental quasiternary CPC at the ternary critical point. Fig. 7 illustrates the procedure. For each quasiternary system, this methodology was applied to the experimental CPC obtained at two different temperatures. With the two calculated χ_{13} values, a $\chi(T)$ equation was estimated for the S–CTBN and S–VTBN systems. Table 2 shows the calculated constants a and b of the $\chi(T)$ equations for all the binary systems studied. Calculated interaction parameters are in the order $\chi(T)_{\text{S–VTBN}} > \chi(T)_{\text{S–CTBN}}$. As in the DMAR–CTBN and DMAR–VTBN quasibinaries, this behavior can be explained through the different chain end groups present in the two rubber molecules.

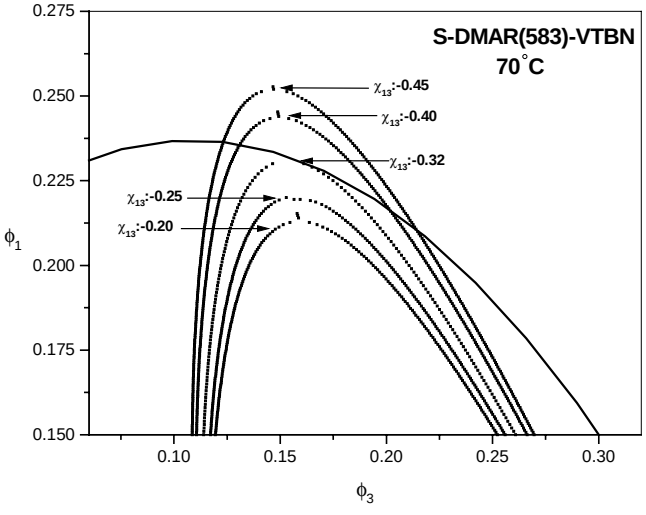

Fig. 7. Sensibility test of the experimental CPC and calculated SC with the S–VTBN interaction parameter. CPC is the best fit to the experimental data of the quasiternary system, S–DMAR(583)–VTBN at 70°C.

4.2. Quasiternary systems

4.2.1. S(1)–DMAR(583)(2)–CTBN(3) and S(1)–DMAR(583)(2)–VTBN(3)

Combination of the required thermodynamic condition for the equilibrium of phases (Eq. (13)), the expression for the chemical potential of an *ij* molecular specie (Eq. (6)) and the mass balance equation for the β phase, allows us to calculate the compositions for the two liquid phases in equilibrium at the cloud-point condition. The locus of these compositions determinate the CPC for the mother phase and the ShC for the emergent phase.

From the equilibrium conditions between the phases (Eq. (13)), three equations can be written, one for each component in the ternary mixture. For the styrene (component 1) the equation is:

$$\sigma_1 - \left[\left(\frac{\phi_1}{r_{1n}} + \frac{\phi_2}{r_{2n}} + \frac{\phi_3}{r_{3n}}\right)^{\beta} - \left(\left(\frac{\phi_1}{r_{1n}} + \frac{\phi_2}{r_{2n}} + \frac{\phi_3}{r_{3n}}\right)^{\alpha}\right)\right] + \chi_{12}[(\phi_2(1-\phi_1))^{\beta} - (\phi_2(1-\phi_1))^{\alpha}] + \chi_{13}[(\phi_3(1-\phi_1))^{\beta} - (\phi_3(1-\phi_1))^{\alpha}] - \chi_{23}[(\phi_2\phi_3)^{\beta} - (\phi_2\phi_3)^{\alpha}] = 0 \quad (19)$$

and similarly, two other equations are written for DMAR(583) and VTBN (or CTBN) components.

The mass balance for the emergent phase is

$$\sum_{j=1}^{N_3} \phi_3^{\alpha} W_{3j} \exp(r_{3j}\sigma_3) + \phi_2^{\alpha}\exp(r_2\sigma_2) + \phi_1^{\alpha}\exp(r_1\sigma_1) = 1. \quad (20)$$

The substitution of the mass balance equations for the mother phase (Eq. (4)) and for the emergent phase (Eq. (20)) in the three equilibrium equations (Eq. (19)) leads to a system of three equations with four unknown variables. If the binary interaction parameters are known at a given temperature, this three equations system (19) can be solved numerically for the unknown independent global compositions, (ϕ_1^{α}, ϕ_2^{α}) and (ϕ_1^{β}, ϕ_2^{β}), assuming one of them as fixed. In this way, the CPC and ShC can be predicted. In the calculations, each polydisperse component was represented by the same distribution function that was used in the analysis of the corresponding quasibinary.

Fig. 8a and b show the experimental data and calculated CPCs, ShCs, SCs and CSPs for the S–DMAR(583)–VTBN quasiternary system at 50 and 70°C, respectively. A good agreement between the experimental and calculated CPCs is obtained. Polydispersity effect can be clearly observed because CPC and ShC are not coincident, although they intercept at the CSP, when both phase compositions are equal.

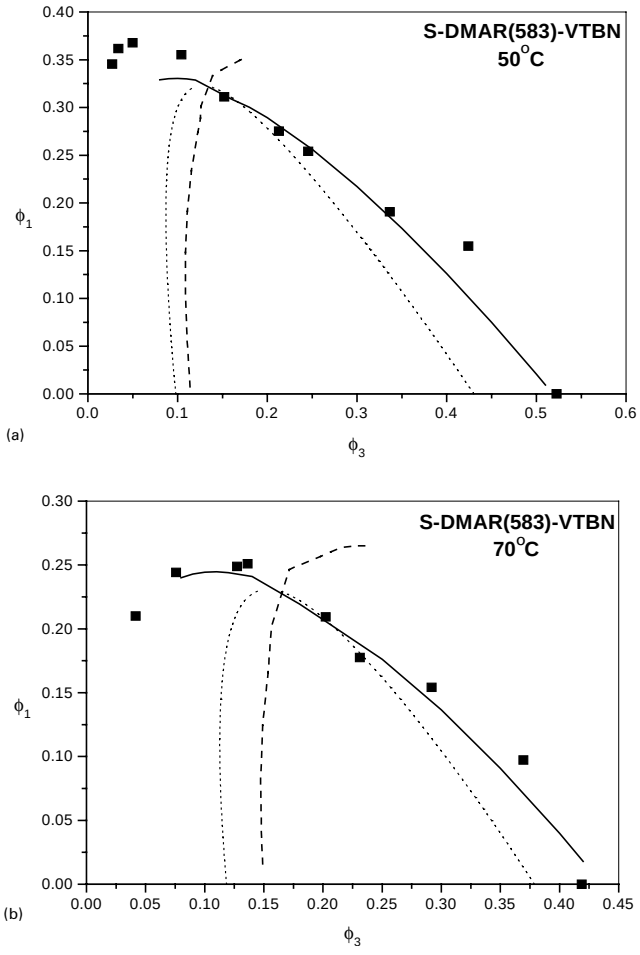

Fig. 8. S–DMAR(583)–VTBN quasiternary system at 50 (a), and 70°C (b); ■ experimental cloud-point data; — calculated cloud-point curve; - - - calculated shadow curve; ⋯ spinodal curve.

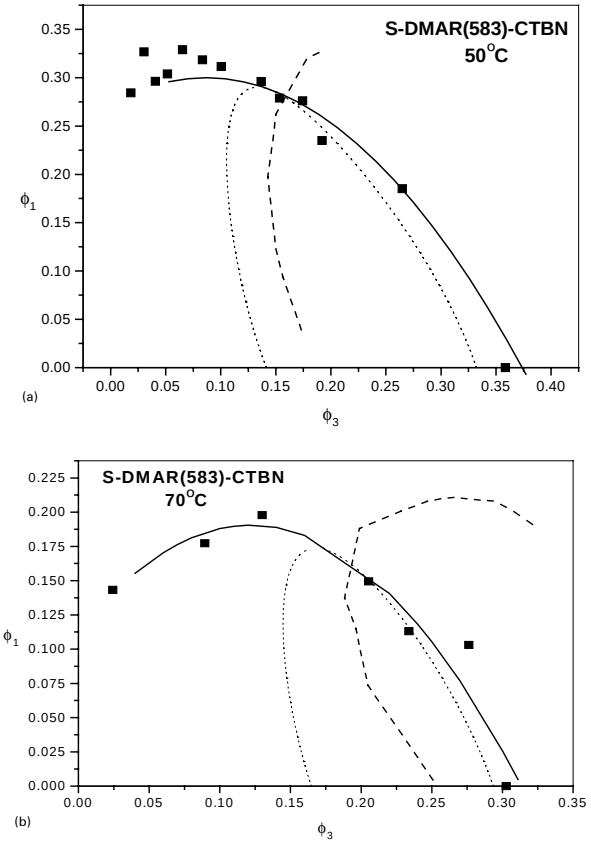

Fig. 9. S–DMAR(583)–CTBN quasiternary system at 50 (a), and 70°C (b); ■ experimental cloud-point data; — calculated cloud-point curve; - - - calculated shadow curve; ⋯ spinodal curve.

Fig. 9a and b show experimental and calculated results for S–DMAR(583)–CTBN quasiternary system at 50 and 70°C, respectively. The general behavior of this system is qualitatively similar to the S–DMAR(583)–VTBN, the only major difference is the higher miscibility showed in the system containing CTBN, in comparison with that containing VTBN. This difference is caused by the higher values of the interaction parameters of the quasibinary systems formulated with VTBN in comparison with those formulated with CTBN.

4.3. Morphologies of the modified materials

Commercial vinyl ester resins are usually formulated to be crosslinked at room temperature (close to 30°C), with cobalt organic salts or amines to promote the cure reactions. Typical concentrations of comonomers and additives in these applications are 40.5%S + 49.5%DMAR + 10%CTBN. Point N in Fig. 10 shows this typical commercial formulation in the corresponding quasiternary phase diagram. Predicted cloud-point phase equilibrium behavior for DMAR(1015) modified system at 30°C is represented by the upper CPC and SC in this diagram, while the behavior of the low molecular weight DMAR (583) formulated system is represented by the bottom curves. The position of point N indicates that the DMAR(583) mixture is homogeneous at this composition,

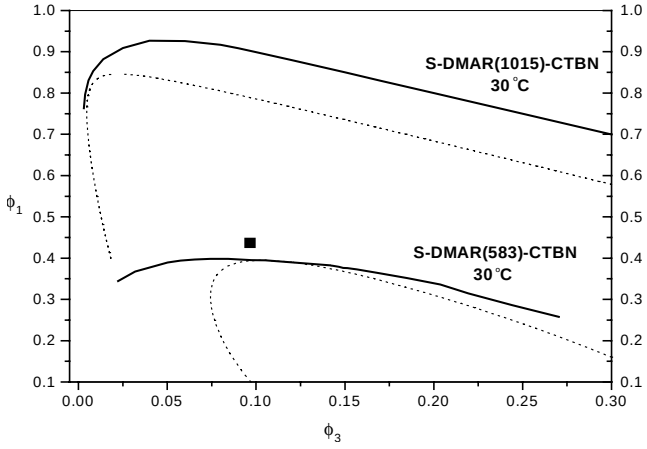

Fig. 10. Calculated quasiternary CPC and SC at 30°C: (a) S–DMAR(1015)–CTBN system; (b) S–DMAR(583)–CTBN system; ■ 40.5%S–49.5%DMAR–10%CTBN sample composition.

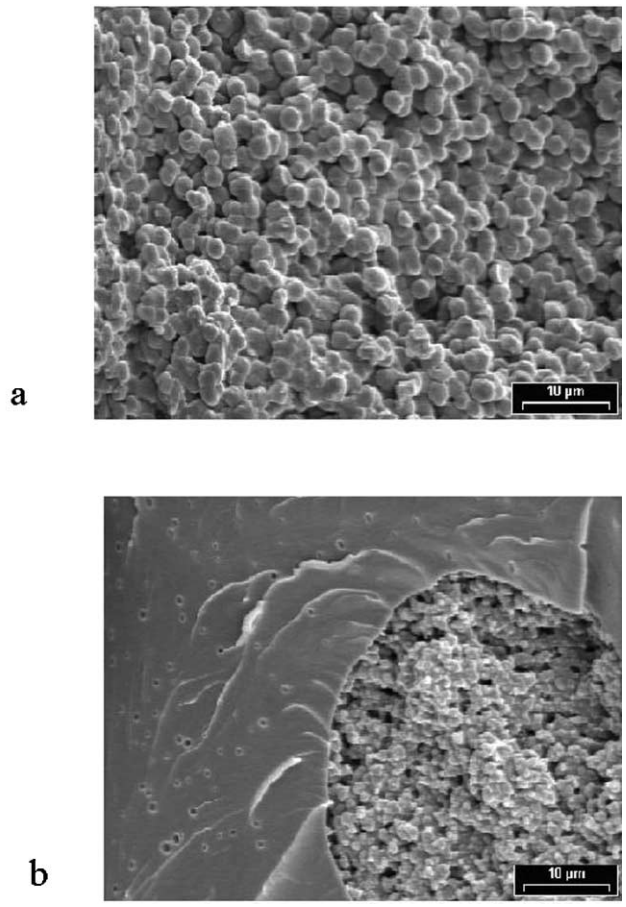

Fig. 11. SEM micrographs of the fracture surface: (a) 40.5%S–49.5%DMAR(583)–10%CTBN sample; (b) 40.5%S–49.5%DMAR (1015)–10%CTBN sample.

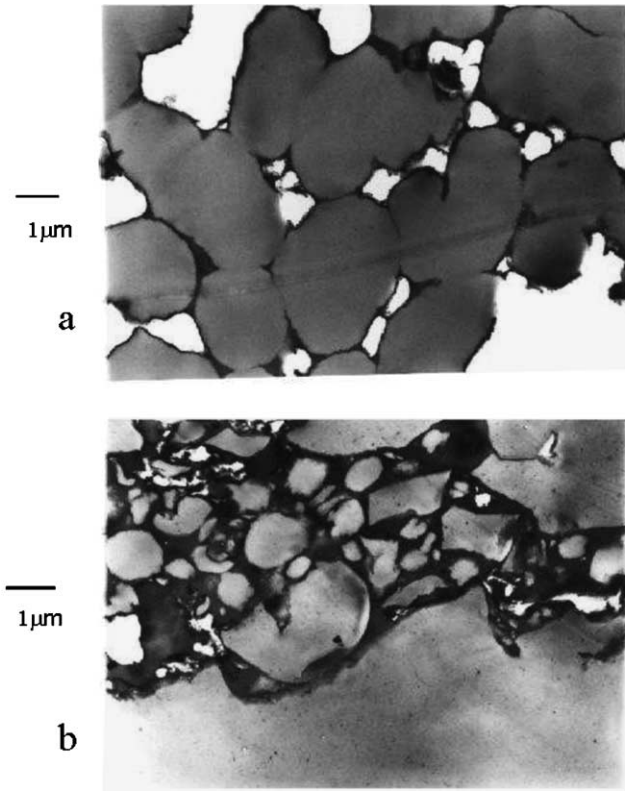

Fig. 12. TEM micrographs of OsO_4 stained fracture surface: (a) 40.5%S–49.5%DMAR(583)–10%CTBN sample; (b) 40.5%S–49.5%DMAR (1015)–10%CTBN sample.

just over the CPC. On the other hand, DMAR(1015) mixture is phase separated even before the curing process, prediction that has been experimentally confirmed, since the unreacted mixture becomes macroscopically separated in two different phases at room temperature. In consequence, the material obtained from the modified DMAR(1015) mixture will be heterogeneous from the beginning of the cure reaction and the final morphology will be greatly dependent on the initial mixing step. Actually, this morphology will be very different from that developed by the DMAR(583) modified system, which is the result of the phase separation originated by the PIPS mechanism from an initial homogeneous solution.

Fig. 11a and b show fracture surfaces (SEM micrographs) of the final cured materials originated from these two reactive quasiternaries, 40.5%S–49.5%DMAR(583)–10%CTBN and 40.5%S–49.5%DMAR(1015)–10%CTBN, respectively. Fig. 12a and b show the TEM micrographs of those same samples, after OsO_4 stainning. These figures show the rubber rich phase as dark gray areas, since the internal rubber double bonds have reacted with OsO_4, while the nodular phase in Fig. 12a and b and the continuous phase in Fig. 12b (poor in CTBN) look light gray [34,35]. White areas in Fig. 12a represent holes or voids in the thin stained sample. The final morphology differences between these two samples have a clear correlation with the initial miscibilities of the unreacted quasiternary systems. The material obtained with DMAR(583) shows an uniform nodular morphology (Fig. 11a) constituted by nodules with diameters in the range of 1–5 μm [34,35]. Nodules are formed by S–DMAR(583) crosslinked copolymer. Surrounding the nodules, there is a continuous minor phase rich in CTBN liquid rubber, as shown by the dark gray areas in Fig. 12a.

Cured materials prepared with DMAR(1015) show large spherical domains surrounded by a continuous phase (Fig. 11b). These domains, with sizes in the range of 20–60 μm and internal nodular microstructure, were originated at the start of the reaction. Initially two separated macrophases are present: the low-density CTBN-rich phase, which will be the minor phase in the final material and the high-density CTBN-poor phase, which will form the majority of the continuous phase. Both separated macrophases could be considered as independent reactors during the curing step. Phase separation process by the PIPS mechanism takes place at different rates in each of the two initially homogeneous macrophases. Inside the spherical domains, rich in the CTBN modifier, a nodular structure is generated in the same way than in the DMAR(583) system (light gray regions in Fig. 12b), with a continuous

phase rich in the rubber component (dark gray regions in Fig. 12b). Outside the domains, the continuous phase undergoes phase separation forming very little, well dispersed CTBN rich spherical particles, as shown in Fig. 11b. The flaky structure of the continuous phase have an aspect very similar to that of the fracture surfaces of the unmodified cured S–DMAR system, which is a brittle material [34,35].

5. Conclusions

Experimental CPCs measurements for the quasibinaries, S–DMAR(1015), DMAR(583)–CTBN and DMAR(583)–VTBN, and the quasiternaries, S–DMAR(583) –CTBN and S–DMAR(583)–VTBN, were used to calculate all the binary interaction parameters according to the F–H lattice theory. Liquid CTBN and VTBN rubbers and DMAR(1015) polydispersities were taken into account in the calculations. Definition of pseudocomponents from DMAR(1015) SEC mass-fraction distribution was an effective method to represent its complex actual distribution. The interaction parameters determined for the binary mixtures allowed us to predict the liquid–liquid phase diagrams of S–DMAR–CTBN (VTBN) ternary mixtures at different temperatures. The predicted phase diagrams give useful information about the initial miscibility of modified S–DMAR systems and allow us to explain major differences between the final complex morphologies of the crosslinked materials.

References

[1] Selly JL. Encyclopedia of polymer science and engineering. 2nd ed., vol. 12. Mark-Bikales-Overberger-Menges: Wiley, 1998.
[2] Zawke SH. In: Goodman De SH, editor. Handbook of thermosetting resins. New Jersey: Noyes Publications, 1986.
[3] Pham S, Burchill PJ. Polymer 1995;36:3279.
[4] Ullett JS, Chartoff RP. Polym Engng Sci 1995;35:1086.
[5] Hsu CP, Kinkelaar M, Hu P, Lee LJ. J Polym 1991;31:1450.
[6] Suspene L, Fourquier Q, Yang YS. Polymer 1991;32:1593.
[7] Lucas JC, Borrajo J, Williams RJJ. Polymer 1993;34:3216.
[8] Cook WD, Zipper MD, Chung ACH. Polymer 1998;39:5431.
[9] Bucknall CB, Partridge IK, Phillips MJ. Polymer 1991;32:786.
[10] Hang YJ, Su CC. J Appl Polym Sci 1995;55:305.
[11] Hang YJ, Su CC. J Appl Polym Sci 1995;55:305.
[12] Huang YJ, Jiang WC. Polymer 1998;39:6631.
[13] Flory PJ. Principles of polymer chemistry. Ithaca, NY: Cornell University Press, 1953.
[14] Tompa H. Polymer solutions. London: Butterworths, 1956. p. 182.
[15] Kamide K. In: Jenkis AD, editor. Thermodynamics of polymer solutions: phase equilibria and critical phenomena, Polymer science library 9. Amsterdam: Elsevier, 1990.
[16] Painter PC, Coleman MM. Fundamentals of polymer science. Lancaster, PA: Technomic, 1994.
[17] Shirataki H, Matsuda S, Kamide K. Br Polym J 1990;23:299.
[18] Shirataki H, Matsuda S, Kamide K. Polym Int 1993;32:265.
[19] Lecointe JP, Pascault JP, Suspène L, Yang YS. Polymer 1992;33:3226.
[20] Borrajo J, Riccardi CC, Williams RRJ. Polymer 1994;35:5541.
[21] Riccardi C, Borrajo J. Polym Int 1993;32:241.
[22] Koningsveld R, CarmÍn HAG, Gordon M. Proc R Soc Lond, A 1970;319:331.
[23] Koningsveld R, Staverman AJ. J Polym Sci, Part A-2 1968;6:306.
[24] Koningsveld R, Staverman AJ. J Polym Sci, Part A-2 1968;6:325–48.
[25] Koningsveld R, Staverman AJ. J Polym Sci, Part A-2 1968;6:349.
[26] Šolc K. Macromolecules 1970;3:665.
[27] Margit T. Rätzsch. Makromol Chem, Macromol Symp 1987;12:101.
[28] Mumby SJ, Sher P. Macromolecules 1994;27:689.
[29] Kamide K, Matsuda S, Shirataki H. Eur Polym J 1990;26:379.
[30] Sechther L, Wynstra J. Ind Engng Chem 1956;48:86.
[31] Aguad ML, Aranguren MI, Borrajo J. J Appl Polym Sci 1997;64:1059.
[32] Borrajo J, Riccardi CC, Moschiar SM, Williams RJJ. In: Keith Riew C, editor. Rubber-toughened plastics, Advances in chemistry series 222. Washington, DC: American Chemical Society, 1989 (Chapter 14).
[33] Borrajo J, Riccardi C, Williams RJJ, Cao ZQ, Pascault JP. Polymer 1995;36:3541.
[34] Aguad ML. Doctoral thesis, National University of Mar del Plata, Argentina, 1999.
[35] Auad ML, Frontini PM, Borrajo J, Aranguren MI. Polymer 2001;42:3723–30.